KINEMATICS, DYNAMICS AND TRAJECTORY GENERATION OF A THREE-LEGGED CLIMBING ROBOT

Tarun Kumar Hazra and Nirmal Baran Hui

Department of Mechanical Engineering, National Institute of Technology, Durgapur, West Bengal, 713209, India

Abstract: In the present paper, an attempt has been made to design a three-legged climbing robot. Each leg of the robot has been considered to have two revolute joints controlled separately by two differential drive motors. Both forward and inverse kinematics analysis have been conducted. The problem of trajectory generation of each joint (both for swing phase and support) has been solved to suit the basic motion laws of Newton's. Dynamic analysis of each link of all the legs has been derived analytically using Lagrange-Euler formulation. Both kinematic and dynamic analysis models of the robot have been tested through computer simulations while the robot is following a straight line path. It is important to mention that the direction of movement of the robot has been considered in the opposite direction of the gravitational acceleration.

1 INTRODUCTION

It is extremely difficult to develop a robot which can manoeuvre freely in rough terrain, specifically in stiff surfaces. There are robots specifically designed to perform pre-defined task and move in a particular terrain. For example, wheel robots are good for flat surface movement over legged robots because of higher speed and less hazard like gate planning. On the other hand, legged robots are preferred in uneven surfaces and for staircase ascending and descending purposes because of relatively better dynamic stability (Song and Waldron, 1989). Therefore, there is a huge demand of a robot, which is capable of manoeuvring all type of landscapes while carrying some pay-load. If it is so, then we can use them for the purpose of surveillance, military operation, exploration etc.

Quite a large number of researchers developed and/or analysed biped (Vukobratovic et al., 1990, Goswami, 1999), quadruped (Koo and Yoon, 1999) and hexapod robots (Barreto et al., 1998, Erden and Leblebicioglu, 2007). There are many advantages of legged robots over the wheeled robots and some disadvantages too. The main disadvantage is that a legged robot needs to plan both its path as well as gait (the sequence of leg movement) simultaneously during locomotion. However, it is extremely difficult job and complexity increases as the number of legs increases. As a result, stable gait generation

of a hexapod robot is more critical than a quadruped robot. On the other hand, hexapod robot is more statically as well as dynamically stable than the quadruped or the biped one. It is because of the fact that for maintaining stability of a multi-legged robot, its projected center of gravity (CG) should lie within its support region, which is a convex hull passing through its supporting feet. As the number of legs reduces, number of supporting feet reduces and the convex hull becomes smaller. Therefore, it is a fertile area of research and many unsolved research problems still exist.

It is also important to mention that research with the robot having odd number of legs is limited. Bretl et al. (2003) have presented a framework for planning the motion of three-legged climbing robots. They have given stress mostly on the development of motion planning strategy. On the other hand, it is necessary to analyze kinematics and dynamics of any robot before assessing its stability or controlling the robot. There exist less number of published article dealing the issues of gait planning and dynamic stability of three-legged robot. It is nevertheless to mention that the work of Bretl et al. (2003) is inspiring in this context. During locomotion, at least one leg must be in swing phase (i.e., ground reaction forces in that leg would be zero) and it results in instability of the robot. This problem becomes highly complex, if it is planned to move in the uneven surface.

Rest of the paper is structured in the following manner. In Section 2, both forward as well as the inverse kinematics of the said robot has been discussed. The foot trajectory planning of the robot has been explained in Section 3 and formulation of the dynamics model has been presented in Section 4. Results are presented and discussed in Section 5. Finally, some concluding remarks have been made and scope for future work has been indicated in Section 6.

2 KINEMATIC MODEL

In this paper, an attempt has been made to develop a suitable model of a planar three legged robot as shown in Figure 1.

Figure 1: A planar three-legged robot.

Following assumptions are considered during the kinematic and dynamic analysis of the robot.

- Links of the robots are made of rigid bodies and their physical properties are considered to be constant,
- The Center of Gravity (CG) of the robot body is assumed to be coincided with the geometrical center of the body,
- During locomotion, trunk of the robot is considered to be parallel to the plane on which the robot will be moving. Also, height between the trunk and maneuvering plane has been considered to be constant equal to h.
- The direction of gravitational acceleration has been considered along the -ve Y-direction of the body attached coordinate frame of the robot.

A possible kinematic posture of the robot model is shown in Figure 2. The robot consists of a trunk of triangular cross section with each side is equal to a and three legs, which are symmetrically distributed around the three sides of the triangular trunk body.

Each leg has two links connected each other and with the trunk by two rotary joints. It is also important to mention that each joint will be controlled separately using differential drive DC servo motors. The Denavit-Hartenberg (D-H) notations (Denavit and Hartenberg, 1955) have been followed in kinematic modeling of each leg. The base frame (Σ_0) is placed at the centroid of the robot. The other frames (Σ_1, Σ_2, Σ_3, Σ_4 etc.) are defined as body frames and are placed at the different joints of the robot. The 'XY' plane has been considered to be parallel to the robot body and the 'Z-axis' of all the joints is made vertical to the robot body. Table 1 shows four D-H parameters of a leg (say, i), namely link length (a_{j-1}), link twist (α_{j-1}), joint distance (d_j) and joint angle (θ_j) by following the concept described in Craig (Craig 1986).
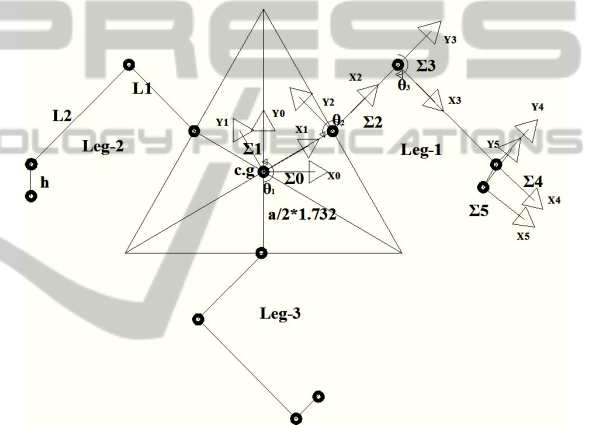

Figure 2: A 2D schematic sketch showing the frames assigned to the first leg of the robot.

Table 1: D-H parameter table for leg-i.

Joint No. (j)	α_{j-1}	a_{j-1}	d_j	θ_j
CG	0	0	0	$\theta_1^{\ i}$
1	0	$a/2\sqrt{3}$	0	$\theta_2^{\ i}$
2	0	L_1	0	$\theta_3^{\ i}$
Tip point	0	L_2	-h	0

It is important to mention that for simplicity, link lengths of all the legs are made same. Therefore, the first link of a leg is denoted by L_1 and second link is represented by L_2. From the above relationship, differences between the coordinates of the foot tip point ($x_{end}^{\ i}$, $y_{end}^{\ i}$, $z_{end}^{\ i}$) and CG (x_c, y_c, z_c) of i-th leg can be determined for the supplied joint variables ($\theta_2^{\ i}$ and $\theta_3^{\ i}$) as follows.

$$\left.\begin{array}{l} p_x{}^i \; = \; (x_{end}{}^i - x_c) \; = \; \dfrac{a}{2\sqrt{3}}c_1{}^i + L_1 c_{12}{}^i + L_2 c_{123}{}^i, \\[2mm] p_y{}^i \; = \; (y_{end}{}^i - y_c) \; = \; \dfrac{a}{2\sqrt{3}}s_1{}^i + L_1 s_{12}{}^i + L_2 s_{123}{}^i, \\[2mm] p_z{}^i \; = \; (z_{end}{}^i - z_c) \; = -h \end{array}\right\} \quad (1)$$

Solving equation (1) algebraically, the joint angles $\theta_2{}^i$ and $\theta_3{}^i$ can be calculated. There will be two solutions for each posture of the robot and two values of $\theta_3{}^i$ can be determined as

$$\theta_{31}{}^i = \text{atan2}\left(s_3{}^i, c_3{}^i\right), \; \text{and} \; \theta_{32}{}^i = \text{atan2}\left(-s_3{}^i, c_3{}^i\right)$$

where $c_3{}^i$ can be found out from the following equation

$$c_3{}^i = \dfrac{\left[\left\{p_x{}^i - \dfrac{a}{2\sqrt{3}}c_1{}^i\right\}^2 + \left\{p_y{}^i - \dfrac{a}{2\sqrt{3}}s_1{}^i\right\}^2 - \left\{L_1{}^2 + L_2{}^2\right\}\right]}{2L_1 L_2} \quad (2)$$

It is important to note that the value of $c_3{}^i$ must lie between -1 and 1 and knowing the values of $\theta_3{}^i$, two values of $\theta_2{}^i$ can be obtained as

$$\theta_{21}{}^i = \text{atan2}\left[\left\{p_y{}^i - \dfrac{a}{2\sqrt{3}}s_1{}^i\right\}, \left\{p_x{}^i - \dfrac{a}{2\sqrt{3}}c_1{}^i\right\}\right] - \varphi_{31}{}^i$$

$$\theta_{21}{}^i = \text{atan2}\left[\left\{p_y{}^i - \dfrac{a}{2\sqrt{3}}s_1{}^i\right\}, \left\{p_x{}^i - \dfrac{a}{2\sqrt{3}}c_1{}^i\right\}\right] - \varphi_{32}{}^i \quad (3)$$

where $\varphi_{31}{}^i = \text{atan2}\left(L_1 s_1{}^i + L_2 \sin\left(\theta_1{}^i + \theta_{31}{}^i\right), L_1 c_1{}^i + L_2 \cos\left(\theta_1{}^i + \theta_{31}{}^i\right)\right)$

$\varphi_{32}{}^i = \text{atan2}\left(L_1 s_1{}^i + L_2 \sin\left(\theta_1{}^i + \theta_{32}{}^i\right), L_1 c_1{}^i + L_2 \cos\left(\theta_1{}^i + \theta_{32}{}^i\right)\right)$

One attempt has been made to find the reachable workspace of the robot. It is graphically obtained in the following manner. Firstly, movement of any two legs was fixed and two links of the other leg is rotated one after another manually and tested how much they can rotate. Angular movement up to which the joints could move before losing its stability provided the reachable workspace. This is important to mention that this test was carried out manually and not optimal in any sense. In the present study solutions belonging to the reachable workspace and lying in non-overlapping zone, have been considered.

3 PLANNING OF JOINT FOOT TRAJECTORY

Motion planning of the robot can be done in three stages (Jamhour and Andre, 1996). During this study, following things are to be satisfied.

(i)　Trajectory should be planned in such a way so that the motion could be maintained smoothly

and uninterruptedly (Mi et al. 2011, Mohri et al. 2001),

(ii)　Joint angle values must satisfy the reachable workspace of the robot.

3.1 Foot Trajectory Generation

In this paper, the joint trajectory is interpolated as a linear function with parabolic blend at the beginning and at the end of the trajectory to consider continuous position and velocity (Craig, 1986).

Let us consider, θ_{oij} and θ_{fij} are the initial and final joint displacements of the j-th link of leg 'i', t_{fij} denotes the time interval of the j-th link of leg 'i' and $\ddot{\theta}_{cij}$ represents the constant acceleration during the blended parabolic trajectory.

For the joint velocities to be continuous, the joint velocity at the end of the first blend must be equal to the beginning of linear segment i. e, at the point (t_{bij}, θ_{ij}), where t_{bij} denotes the time where first blend will occur. Therefore, it must satisfy the following equation.

$$t_{bij} = \left(\tfrac{1}{2} \times t_{fij}\right) - \tfrac{1}{2}\sqrt{\dfrac{\ddot{\theta}_{cij} \times t_{fij}{}^2 - 4 \times (\theta_{fij} - \theta_{0ij})}{\ddot{\theta}_{cij}}} \; \text{and}$$

$$\left|\ddot{\theta}_{cij}\right| \geq \dfrac{4 \times \left|\theta_{fij} - \theta_{0ij}\right|}{t_{fij}{}^2} = K \dfrac{4 \times \left|\theta_{fij} - \theta_{0ij}\right|}{t_{fij}{}^2} \quad (4)$$

The value of K must be greater than unity and in the present study it has been considered to be equal to 1.05. Finally, joint angle expression is presented in equation (5) and joint speed and accelerations are derived by differentiating equation (5) with respect to time.

Joint Angle:

$$\theta_{ij} = \begin{cases} \theta_{0ij} + \dfrac{1}{2}\ddot{\theta}_{cij}(t_{fij})^2, & \text{for} \to 0 \leq t \leq t_{bij} \\[2mm] \theta_{0ij} - \dfrac{1}{2}\ddot{\theta}_{cij}(t_{bij})^2 + \ddot{\theta}_{cij}t_{bij}t, & \text{for} \to t_{bij} < t \leq (t_{fij} - t_{bij}) \\[2mm] \theta_{fij} - \dfrac{1}{2}\ddot{\theta}_{cij}(t_{fij} - t)^2, & \text{for} \to (t_{fij} - t_{bij}) < t \leq t_{fij} \end{cases} \quad (5)$$

3.2 Gait Planning Strategy

The tripod robot model is shown in Figure 1. During locomotion, a one-step movement is normally followed by human being and Bretl et al. (2003) have mentioned that one step movement can also be used for planning gaits of three-legged robots. In the present work the gaits of the robot have also been planned in the similar manner. It has been assumed that during movement at a time only one leg will be in swing phase and other two will be in support

phase. At first say leg-2 and leg-3 are in support phase and leg-1 is in the swing phase moving along a specified path. When leg-1 will reach to its goal configuration, leg-1 and leg-3 will switch to support phase, and leg-2 will be in swinging phase. Thereafter, leg-3 will be in swing phase and the other two will be in support phase. In this way the tip of legs of the tripod reach to the new position with different configurations and completes one locomotion cycle.

Let us say, initial position of the geometric center of the robot is (x_c, y_c, z_c). The CG of the robot is moving in a straight line path along 'Y' axis with a constant speed. The time for a full locomotion cycle is considered to be equal to Δt. After Δt time interval the new position of the CG is $(x_c, y_c + \Delta y, z_c)$. The above movement is achieved in three stages. For each stage, coordinates of the CG of the robot, foot tip point of three legs at different instant of time have been presented in Table 2.

Table 2: Positions of different parts of the robot at four instant of time of a locomotion cycle.

Time ($t = k\Delta t$)	CG	Foot tip point		
		1st leg	2nd leg	3rd leg
k=0	x_c, y_c, z_c	x_1, y_1, z_1	x_2, y_2, z_2	x_3, y_3, z_3
k=1/3	$x_c, (y_c + \Delta y / 3), z_c$	$x_1, (y_1 + \Delta y), z_1$	x_2, y_2, z_2	x_3, y_3, z_3
k=2/3	$x_c, (y_c + 2\Delta y / 3), z_c$	$x_1, (y_1 + \Delta y), z_1$	$x_2, (y_2 + \Delta y), z_2$	x_3, y_3, z_3
k=1	$x_c, (y_c + \Delta y), z_c$	$x_1, (y_1 + \Delta y), z_1$	$x_2, (y_2 + \Delta y), z_2$	$x_3, (y_3 + \Delta y), z_3$

4 DYNAMICS OF THE ROBOT

Dynamics of different kind of robot have been explained in (Mi et al. 2011, Mohri et al. 2001). In the present paper, Lagrangian Euler-based formulation has been used. Torque expression for first joint of i-leg can be derived as follows.

$$
\tau_{i1} = \left[\frac{13}{12} m_1 L_1^2 + m_2 L_1^2 + \frac{13}{12} m_2 L_2^2 + 2 m_2 L_1 L_2 c^i_3 \right] \ddot{\theta}^i_2
$$
$$
+ \left[\frac{13}{12} m_2 L_2^2 + m_2 L_1 L_2 c^i_3 \right] \ddot{\theta}^i_3 + \left[\begin{matrix} (m_1 + m_2) L_1 c^i_{12} \\ + m_2 L_2 c^i_{123} \end{matrix} \right] \ddot{y}_c
$$
$$
- m_2 L_1 L_2 s^i_3 \dot{\theta}^i_3 \left(2\dot{\theta}^i_2 + \dot{\theta}^i_3 \right) + \frac{1}{2} m_1 g L_1 c^i_{12} \qquad (6)
$$
$$
+ \frac{1}{2} m_2 g L_2 c^i_{123} + m_2 g L_1 c^i_{12} + M^i_F
$$

Similarly, for second joint of each leg torques can be calculated using the expression

$$
\tau_{i2} = \left[\frac{13}{12} m_2 L_2^2 + m_2 L_1 L_2 c^i_3 \right] \ddot{\theta}^i_2 + \left[\frac{13}{12} m_2 L_2^2 \right] \ddot{\theta}^i_3
$$
$$
+ \left[m_2 L_2 c^i_{123} \right] \ddot{y}_c + \left[m_2 L_1 L_2 s^i_3 \dot{\theta}^{i\,2}_2 \right] + \qquad (7)
$$
$$
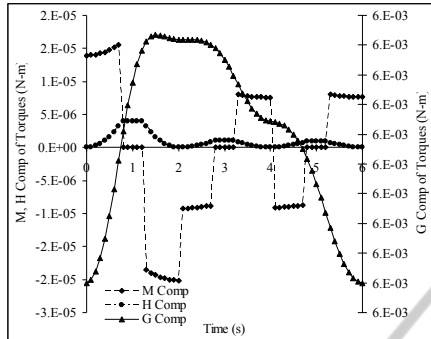\left[\frac{1}{2} m_2 g L_2 c^i_{123} \right] + M^i_F
$$

Here, m_1 and m_2 denote mass of links 1 and 2, respectively. Acceleration due to gravity is represented by g, speed of the CG of the robot is denoted by $\ddot{y}_c$ and M^i_F represents the torque due to foot reaction forces at i-th Leg and it is zero for the leg which is in swing phase. It is important to mention that all the joint torque expressions have been derived with respect to the coordinated frame attached to the CG of the robot. The value of g is considered to be equal to $\begin{bmatrix} 0 & -9.81 & 0 \end{bmatrix} m/s^2$.
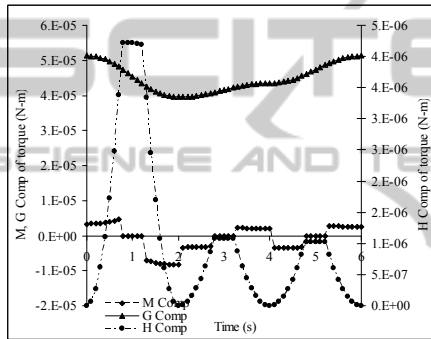
5 SIMULATION RESULTS

Developed mathematical models have been tested through computer simulations. In the present case, the leg stroke of the one step movement (Δy), body height (h), side length of the triangular-shaped cart (a) and time step are assumed to be equal to 0.03m, 0.05m, 0.12m and 6 seconds, respectively. During analysis, following data have been considered: L_1=0.04m, L_2=0.06m, m_1=0.002Kg, m_2=0.012Kg, coordinates of CG (0,0,0.05)m, foot tip points during starting for the first leg (0.09,0.05,0)m, for the second leg (-0.09,0.05,0)m and third leg at (0.01,-0.11,0)m.

It is important to mention that forward kinematics always leads to a single pose matrix for any robot. However, several robot configurations (i.e., joint angle values) may result in the same foot tip point corresponding to a fixed location of the CG. In the present study, two solutions are obtained that will generate the same foot tip point of the robot. It provides freedom in the trajectory planning. In the present study, only those combinations of solutions have been preferred, which are falling within the reachable workspace of the robot. Maximum joint angle speed and acceleration values at different instant of time for legs 1, 2 and 3 are calculated and it has been observed that those values are higher during swing phase than the support phase. It may be due to the absence of support reaction forces during swing phase.
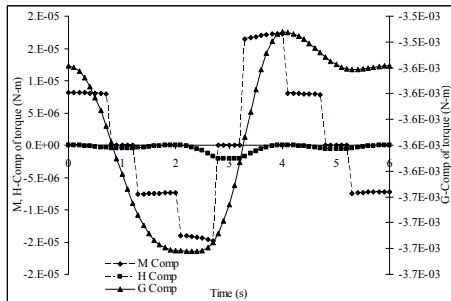
From equations (6) and (7), it is clear that joint torques is comprised of three components: inertial (M Comp), centrifugal and/or Coriolis (H Comp) and Gravity (G Comp) (refer to Figure 3).
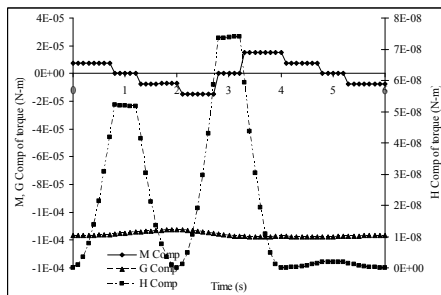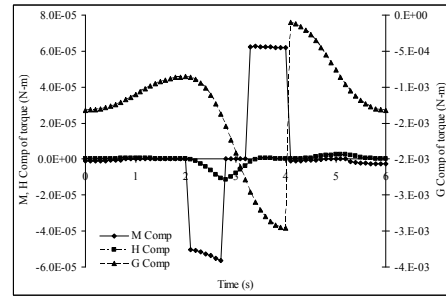
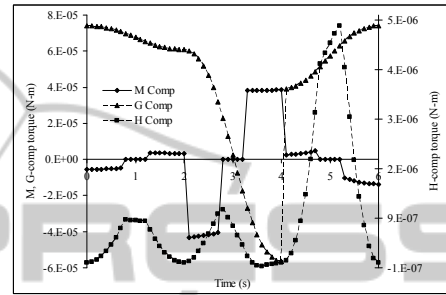(a) Joint 1 of Leg-1.

(b) Joint 2 of Leg-1.

(c) Joint 1 of Leg-2.

(d) Joint 2 of Leg-2.

(e) Joint 1 of Leg-3.

(f) Joint 2 of Leg-3.

Figure 3: Contribution of M-comp, H-comp and G-comp of on the joint torques over the entire locomotion cycle.

During this study, following common observations are made.

(i) During the first 1/4-th and last 1/4-th time period of every stages of locomotion cycle, inertial component of torque has been found to be approximately constant and in-between it is observed to be zero. It is because of the acceleration distributions considered in the study. That is why, it is almost constant for second joint, whereas it is varying little bit for the first joint. These small variations might have occurred due to the contributions from the other joints.

(ii) **For the First Joint:** Contribution of gravity component in all the legs has been found to be more compared to the other two components. Gravity component has been observed to be varying in the positive side only for Leg 1. On the other hand it is varying both in positive as well as in negative side for the other two legs. It clearly indicates that the requirement of torque for the first leg is more in compared to the other legs.

(iii) **For the Second Joint:** Contribution of centrifugal and/or Coriolis component in all the legs is observed to be very low. It might be due to the fact that first joint does not have any contribution on this component of torque.

Total torque requirement for the first joint of

every leg has been found to be more in compared to the second joint. Moreover, for controlling of first joint of Leg 1, torque requirement is observed to be considerably higher than the other legs. It is also to be noted that torque requirement for each joint during swing phase is less in compared to the support phase. This is because of the presence of support reaction forces.

6 CONCLUDING REMARKS

This paper presented kinematics, dynamics and trajectory planning of a three-legged robot. Direct and inverse kinematics has been analyzed, while the robot is following a straight line path. Movement of the robot is ensured considering that at any instant of time only one leg can be in swing phase while the other two will provide necessary support. Joint torques has been computed continuously for the full locomotion cycle and compared between the legs. All the developed mathematical models have been tested through computer simulations on a P-IV PC. Computational complexity of the code developed for solving the mathematical expressions is found to be very low, making it suitable for on-line implementations. More torque requirement has been observed for the first joint of each leg and for every joint during support phase than in swing phase. For the first joint of each leg, torques varies between (-0.004N-m to 0.00585N-m) and those for the second joint vary between (-0.00003N-m to 0.00007N-m). This is a very low torque requirement and low power servo motors will be sufficient to control them.

The present study can be extended in a number of ways, such as, static and dynamic stability analysis, optimization of joint torques of the robot while it is following a curvilinear path. Moreover, presently the performance of the robot has been tested through computer simulations. Real experiments will be more interesting in this regard. The authors are working with some of these issues presently.

REFERENCES

Barreto J. P., Trigo A., Menezes P., Dias J., 1998. Almeida A. T. D, FBD-the free body diagram method. Kinematics and dynamic modeling of a six leg robot, *IEEE Int. Conf. on Robotics and Automation*, pp. 423-428

Bretl T., Rock S., Latombe J. C., 2003. Motion planning for a three-limbed climbing robot in vertical natural terrain, *in Proc. IEEE Intl. Conf. on Robotics and Automation, Taipai, Taiwan*

Craig J. J., 1986. Introduction to robotics: mechanics and control, Addison-Wesley, Singapore

Denavit J., Hartenberg R. S., 1955. A kinematic notation for lower-pair mechanisms based on matrices, *ASME Journal of Applied Mechanics*, Vol. 77, pp. 215-221

Erden M. S., Leblebicioglu K., 2007. Torque distribution in a six-legged robot, *IEEE Trans. on Robotics*, vol. 23(1), pp. 179-186

Goswami A., 1999. Foot rotation indicator point: a new gait planning tool to evaluate postural stability of biped robots, in: *Proc. of the IEEE Int. Conf. on Robotics and Automation*, Detroit, USA, vol. 1, pp. 47–52

Jamhour E., Andre P. J., 1996. Planning smooth trajectory along parametric paths, Mathematics and Computers in Simulation, vol. 41, pp. 615-626

Koo T. W., Yoon Y. S., 1999. Dynamic instant gait stability measure for quadruped walking, Robotica, vol. 17, pp. 59-70

Mi Z., Yang J., Kim J. H., Abdel-Malek K., 2011. Determining the initial configuration of uninterrupted redundant manipulator trajectories in a manufacturing environment, *Robotics and Computer-Integrated Manufacturing*, vol. 27, pp. 22-32

Mohri A., Furuno S., Yamamoto M., 2001. Trajectory planning of mobile manipulator with end–effectors specified path, *in Proc. of the Intl. Conf. on Intelligent Robots and Systems*, Maui, Hawali, USA, pp. 2264-2269

Song S. M. and Waldron K. J., 1989. Machines that walk: the adaptive suspension vehicle, *The MIT Press, Cambridge*, Massachusetts

Vukobratovic M., Borovac B., Surla D., Stokic D., 1990. Biped locomotion-dynamics, stability, control and applications, Springer-Verlag.